Acta Crystallographica Section F
**Structural Biology and Crystallization Communications**
ISSN 1744-3091

# Structure of a pectin methylesterase from *Yersinia enterocolitica*

**Alisdair B. Boraston[a] and D. Wade Abbott[b]***

[a]Department of Biochemistry and Microbiology, University of Victoria, PO Box 3055 STN CSC, Victoria, BC V8W 3P6, Canada, and [b]Lethbridge Research Station, Agriculture and Agri-Food Canada, 5403 1st Avenue South, Lethbridge, AB T1J 4B1, Canada

Correspondence e-mail: wade.abbott@agr.gc.ca

Received 2 December 2011
Accepted 23 December 2011

**PDB Reference:** pectin methylesterase, 3uw0.

Pectin methylesterases (PMEs) are family 8 carbohydrate esterases (CE8s) which remove the methyl group from methylesterified galacturonic acid (GalA) residues within pectin. Although the role of pectinases such as PMEs within dedicated phytopathogens has been well established, the significance of homologous enzymes found within the genomes of human enteropathogens remains to be determined. Presented here is the low-resolution (3.5 Å) structure of the CE8 from *Yersinia enterocolitica* (*Ye*CE8). The high degree of structural conservation in the topology of the active-site cleft and catalytic apparatus that is shared with a characterized PME from a bacterial phytopathogen (i) indicates that *Ye*CE8 is active on methylated pectin and (ii) highlights a more prominent role for pectin utilization in *Yersinia* than in other enteropathogenic species.

## 1. Introduction

Family 8 carbohydrate esterases (CE8s) are a group of sequence-related enzymes found within the domains Archaea, Bacteria and Eukarya (http://www.cazy.org; Cantarel *et al.*, 2009). Currently, 40 different CE8s have been characterized as pectin methylesterases (PMEs), enzymes which remove the methyl group from methyl-esterified galacturonic acid (GalA) residues within pectin. This is a significant biological event in processes such as cell-wall turnover, fruit ripening and pathogenesis. Removal of methanol from a methyl-esterified GalA (*i.e.* demethoxylation, referred to below as demethylation) restores the inherent negative charge on the uronate group of GalA, which loosens the higher order structure of the pectic network through electrorepulsive effects (Pelloux *et al.*, 2007). In bacteria, two different isozymes have been described, PmeA/PemA (pectin methylesterase A) and PmeB/PemB (pectin methylesterase B), both of which are required for optimal growth of the phytopathogen *Dickeya dadantii* 3937 (formerly *Erwinia chrysanthemi* 3937) on highly methylated pectic substrates (Shevchik *et al.*, 1996). PmeA is a secreted PME that is active on highly polymerized methylated pectin and is closely related to plant PMEs, whereas PmeB belongs to a smaller subfamily of PMEs that are specific for methylated oligogalacturonides and are lipid-anchored to the periplasmic face of the outer membrane (Shevchik *et al.*, 1996; Kazemi-Pour *et al.*, 2004). These two distinct profiles suggest unique roles for each isozyme along the pectinolytic cascade. In eukaryotes, a separate nomenclature has been adopted in which pectin methylesterase isozymes are delineated numerically (*i.e.* Pme1, Pme2). Below, enzymes will be identified using the CAZy classification system, which consists of the italicized initials of the host species followed by the enzyme family (*i.e.* the PME from *Yersinia enterocolitica* is *Ye*CE8).

Recently, a role other than demethylesterification of pectin has been suggested for a small subclade of CE8s (Eklöf *et al.*, 2009). The YbhC gene product from *Escherichia coli* K-12 MG1655 (*Ec*CE8) does not display any esterase activity on highly methylated polygalacturonic acid, nor does it interact with this polymer in binding studies. Structural analysis indicated that *Ec*CE8 contains several

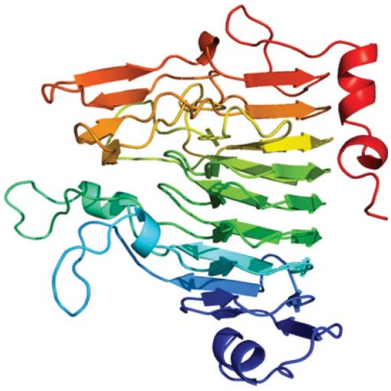

unique motifs: a remodelled active-site cleft with several loop insertions and mutations to key catalytic residues, including the primary general acid–base catalyst (see Supplementary Material[1]). Intriguingly, phylogenetic analysis of *Ec*CE8 indicated that a cluster of enzymes belonging to enteric bacteria, such as *Enterobacter*, *Klebsiella*, *Salmonella* and *Shigella*, appear to have evolved from a common PmeB ancestor (Eklöf *et al.*, 2009). Previously, the exclusive role of CE8s in pectin degradation suggested that this enzyme was a highly conserved member of a pectin-utilization pathway found in a number of foodborne pathogens from Enterobacteriaceae (Rodionov *et al.*, 2004; Abbott & Boraston, 2008). The relationship now however appears to be more biologically complex. Therefore, in order to further explore the role of CE8s in Enterobacteriaceae, the homologue from *Y. enterocolitica*, *Ye*CE8, has been cloned and structurally characterized at low resolution (3.5 Å). The complex evolutionary history of the emergence of pectin-utilization systems within enteropathogens is discussed.

## 2. Materials and methods

### 2.1. Cloning, production and purification of recombinant *Ye*CE8

The gene sequence of *Ye*CE8 (locus tag Ye0549), without the N-terminal 25-amino-acid signal peptide, was amplified from the genomic DNA of biotype O:8, serotype 1B *Y. enterocolitica* subsp. *enterocolitica* 8081 (ATCC ID No. 27729D-5). An in-frame 5′ *Nhe*I restriction site, encoded within the primer sequence ATAT**GCTAGC**GCGCAGTATAATGCAGTTGTTTCT, and 3′ *Xho*I restriction site, encoded within the primer sequence ATAT**CTCGAG**TCAATGCACGGCCCAATCAGGGAA, were introduced into the PCR product for directional cloning. The amplicon was purified, digested and ligated into pET28a plasmid vector (Novagen, catalogue No. 69864) treated with complementary enzymes. The generated expression construct, pYECE8, contained a thrombin-cleavable N-terminal $His_6$ tag (MGSSHHHHHHSSG**LVPR–GS**HM). Ligated vectors were subsequently transformed into DH5$\alpha$ competent cells for propagation. Positive clones were purified and verified by restriction digest and DNA sequencing.

Recombinant *Ye*CE8 protein was produced in *E. coli* BL21 (DE3) (Novagen, catalogue No. 69041). Transformed cells were grown at 310 K with shaking at 180 rev min$^{-1}$ in LB supplemented with 50 µg ml$^{-1}$ kanamycin to an OD of ∼0.8 at 600 nm. At this density, the temperature was decreased to 289 K for 1 h with shaking; gene expression was then induced using 0.2 m*M* isopropyl $\beta$-D-1-thiogalactopyranoside with shaking overnight. The following morning, the cells were harvested by centrifugation at 6000*g* and disrupted by chemical lysis. Following clarification by centrifugation at 15 000*g*, *Ye*CE8 was purified by immobilized metal-affinity chromatography using Ni-Sepharose resin (GE Healthcare, catalogue No. 17-5318-06) equilibrated in 500 m*M* sodium chloride, 20 m*M* Tris–HCl pH 8.0. Bound protein was eluted with a stepwise gradient from 0 to 500 m*M* imidazole in the aforementioned buffer. Protein fractions were analyzed for purity by SDS–PAGE and samples containing appreciable amounts of pure *Ye*CE8 were pooled and buffer-exchanged to remove imidazole using a stirred-cell ultrafiltration device with a 5000 MWCO membrane (Millipore, catalogue No. PLCC02510). Calcium ions were added to a final concentration of 2 m*M* and the N-terminal six-histidine tag was removed using restriction-grade thrombin (Novagen, catalogue No. 69671). After complete digestion, *Ye*CE8 was further purified by gel-filtration chromatography using a Sephacryl S-200 column (GE Biosciences, catalogue No. 17-0584-05) in 20 m*M* Tris–HCl pH 8.0. Purified polypeptides were concentrated to 20 mg ml$^{-1}$ for crystallization trials, as determined using a calculated extinction coefficient of 1.20 mg ml$^{-1}$ (Gasteiger *et al.*, 2005).

**Table 1**
Data-collection and structure statistics.

Values in parentheses are for the highest resolution shell.

| | |
|---|---|
| Data collection | |
| Wavelength (Å) | 1.1 |
| Space group | $P4_332$ |
| Molecules per asymmetric unit | 1 |
| Solvent content (%) | 76.3 |
| Unit-cell parameters (Å) | $a = b = c = 170.6$ |
| Resolution (Å) | 40.00–3.50 (3.69–3.50) |
| $R_{merge}$ | 0.17 (0.60) |
| $\langle I/\sigma(I)\rangle$ | 21.2 (5.9) |
| Completeness (%) | 99.9 (99.9) |
| Multiplicity | 24.7 (21.1) |
| Mosaicity (°) | 0.89 |
| No. of crystals | 1 |
| Temperature (K) | 100 |
| Oscillation (°) | 1 |
| Rotation range (°) | 129 |
| Exposure per frame (s) | 20 |
| Crystal-to-detector distance (mm) | 200 |
| Detector | CCD |
| Refinement | |
| No. of reflections | 10653 |
| $R_{work}/R_{free}$ | 0.20/0.25 (0.18/0.26) |
| No. of atoms | |
| Protein | 2409 [chain *A*] |
| Water | 13 [chain *B*] |
| *B* factors (Å$^2$) | |
| Protein | 59.9 |
| Water | 36.2 |
| R.m.s. deviations | |
| Bond lengths (Å) | 0.0048 |
| Bond angles (°) | 0.92 |
| Ramachandran plot (%) | |
| Favoured | 95.6 |
| Allowed | 4.4 |
| Outliers | 0.0 |

### 2.2. *Ye*CE8 crystallization conditions and structure solution

Repeated attempts to crystallize *Ye*CE8 were performed using commercially available crystal screens and the hanging-drop vapour-diffusion method at 291 K. Despite these efforts, no promising crystallization conditions were detected within a period of three months with routine surveillance. After a period of approximately one year the plates were rechecked and a single crystal was observed in a well containing unbuffered 4 *M* sodium formate (condition No. 33 of Crystal Screen; Hampton Research, catalogue No. HR2-110). The crystal was flash-cooled directly in a cryostream at 113 K as the high salt concentration acted as an effective cryoprotectant. Crystallized *Ye*CE8 was verified for X-ray diffraction and data were collected on beamline X8-C at the National Synchrotron Light Source, Brookhaven National Laboratories. Data were processed with *MOSLFM* (Battye *et al.*, 2011), *POINTLESS* (Evans, 2006) and *SCALA* (Evans, 2006) to a resolution of 3.5 Å (Table 1).

The structure of *Ye*CE8 was solved using the *MOLREP* automated molecular-replacement program (Vagin & Teplyakov, 2010) with PmeA from *D. dadantii* 3937 (referred to as *Dd*CE8 below; PDB entry 1qjv; 59% identity over 335 amino acids; Jenkins *et al.*, 2001) as a search model. One molecule was found in the asymmetric unit. Successive rounds of rigid-body and restrained refinement using *REFMAC* (Murshudov *et al.*, 2011) and manual model building in *Coot* (Emsley & Cowtan, 2004) were performed to complete the model. 5% of the reflections were flagged as 'free' and were used to

[1] Supplementary material has been deposited in the IUCr electronic archive (Reference: HV5208).

monitor refinement progress. All waters were added manually based upon difference maps and acceptable distances from local amino acids (2.5–3.5 Å). Validation of the *Ye*CE8 structure was performed using *MolProbity* (Chen *et al.*, 2010) and the resulting statistics are provided in Table 1. Structural alignments were performed with *Coot* (Emsley & Cowtan, 2004). *PyMOL* (DeLano, 2002) was used for figure generation and secondary-structure analysis.

## 3. Results and discussion

### 3.1. The crystal structure of *Ye*CE8

Family 8 carbohydrate esterases adopt a right-handed $\beta$-helix (Fig. 1*a*), which is a common scaffold for a variety of unrelated pectinase families, including polygalacturonases and rhamnogalacturonases (GH28) and pectin and pectate lyases (PL1, PL3 and PL9) (Abbott & Boraston, 2008; Jenkins & Pickersgill, 2001). A prominent cleft is visible on the surface of *Ye*CE8 which is conserved in all structurally characterized PmeAs (Fig. 1*b*; Fries *et al.*, 2007; Jenkins *et al.*, 2001). The open cleft provides the enzyme with access to internal methylations along the length of pectic polymers. The model includes residues 41–360 of the *Ye*CE8 primary structure; a portion of the N-terminus was too disordered to model accurately. In addition to the 2409 protein atoms (chain *A*), 13 water atoms (chain *B*) were added manually on the basis of their proximity to neighbouring side chains (2.5–3.5 Å). Although this structure was solved to a low resolution (3.5 Å), the high redundancy improved the electron-density quality (Fig. 1*c*) and enabled the majority of side-chain fitting to be performed using automated refinement. However, some regions required careful inspection and side-chain truncations were introduced where required to improve the refinement statistics. In areas of ambiguous electron density, manual model building was directed by superimposition with the *Dd*CE8 structure (Jenkins *et al.*, 2001).

A *DaliLite* search (v.3; Holm & Rosenström, 2010) for *Ye*CE8 produced the highest matches with a series of *Dd*CE8 complexes and its apo structure (Fries *et al.*, 2007; Jenkins *et al.*, 2001). Consistent *Z* values were observed in the range 50.2–50.7 and r.m.s.d.s were in the range 0.7–0.9 Å over 319 aligned $C^{\alpha}$ atoms for each chain of these deposited structures. The similar values observed for the complexed and apo forms underlines that these enzymes are rigid and do not display significant conformational changes in the active-site cleft or along the $\beta$-helix backbone following substrate binding. The two

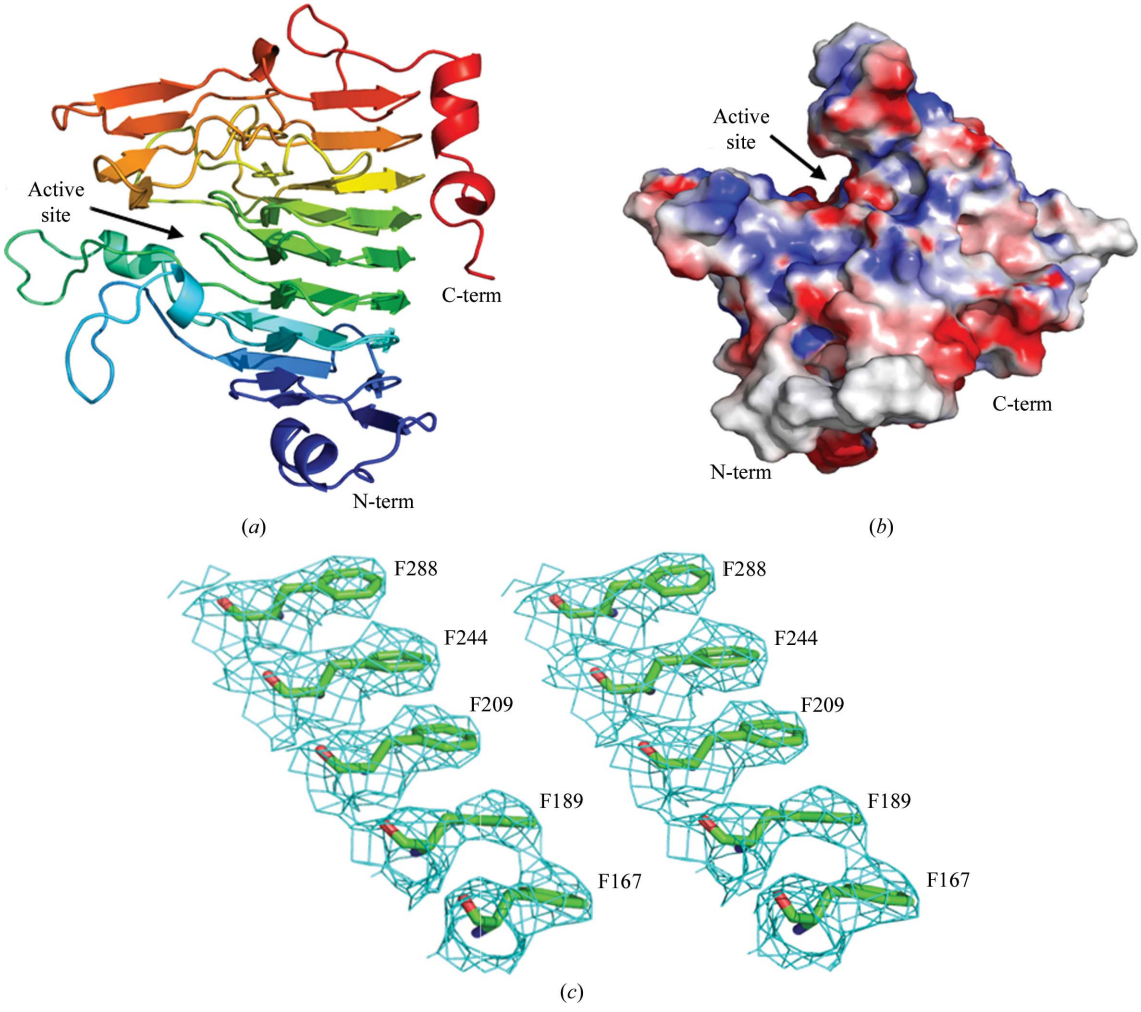


**Figure 1**
The crystal structure of *Ye*CE8. (*a*) Cartoon representation of the *Ye*CE8 $\beta$-helix fold coloured in a rainbow gradient from blue (N-terminus) to red (C-terminus). (*b*) Electrostatic surface potential of *Ye*CE8, highlighting the prominent active-site cleft. (*c*) Wall-eyed representation of the electron density for *Ye*CE8 at 3.5 Å resolution. The maximum-likelihood (Murshudov *et al.*, 2011) $\sigma_A$-weighted (Read, 1986) $2F_{obs} - F_{calc}$ map (coloured in cyan) is contoured at 1.0$\sigma$ (0.11 $e^{-}$ Å$^{-3}$). The internal aromatic stack of phenylalanine residues is a structural feature found in other $\beta$-helix proteins that serves to anchor neighbouring $\beta$-strands and stabilize the overall fold (Jenkins & Pickersgill, 2001).

eukaryotic PMEs from *Solanum lycopersicum* (PDB entry 1xg2; Di Matteo *et al.*, 2005; 25% identity) and *Daucus carota* (PDB entry 1gq8; Johansson *et al.*, 2002; 28% identity) were the next two closest results, with *Z* values of 35.0 and 33.8 and r.m.s.d. values of 1.8 Å over 317 and 319 $C^{\alpha}$ atoms, respectively. YbhC, a PmeB-like homologue from *E. coli* K-12 with unknown activity (PDB entry 3grh; Eklöf *et al.*, 2009; 25% identity), followed the PMEs with a *Z* value of 31.5 and an r.m.s.d. of 1.6 Å over 326 $C^{\alpha}$ atoms. Alignments with pectinases that display distinct activities and low primary-structure identities (<15%) were also observed (r.m.s.d. values of 2.8–3.7 Å), highlighting the flexibility of the $\beta$-helix scaffold in diverse pectinolytic functions.

### 3.2. The *Ye*CE8 active site

A closer look at the core active site of *Ye*CE8 superimposed with the *Dd*CE8–$GalA_6$ complex (PDB entry 2ntb; Fries *et al.*, 2007) indicates that *Ye*CE8 is a PME (Fig. 2). *Ye*CE8 side chains make direct sugar contacts with the oligogalacturonide in five different subsites (labelled −2 to +3 from the nonreducing end; Fig. 2*a*). The scissile GalA methyl group is positioned in subsite +1. The terminal sugar residue at the nonreducing end does not display any direct interactions with the enzyme. Every key residue identified in the *Dd*CE8 enzyme is absolutely conserved; the only subtle difference detected is that the uronate group of GalA in subsite −2 is positioned to make a hydrogen bond to the peptidyl N atom of Ser109 in *Ye*CE8, which replaces the interaction with the peptidyl N atom of Ala110 observed in *Dd*CE8. Significantly, the catalytic triad consisting of Gln176, Asp177 and Asp199 is strictly conserved, with the putative acid–base catalyst Asp177 within hydrogen-bonding distance of O6 of the substrate (Asp177 $O^{\delta1}$ and $O^{\delta2}$ are 2.5 and 3.5 Å from the O6A and O6B atoms of the +1 GalA, respectively). These observations strongly support the contention that *Ye*CE8 and *Dd*CE8 have analogous biological functions in the demethylesterification of pectin.

The recently reported structure of the PmeB-like homologue YbhC from *E. coli* K12 (PDB entry 3grh) provides further clues to the functional specificity of *Ye*CE8. Comparing the global folds of the two subclasses of PMEs previously revealed that the 'closing off' of one end of the active site by loop insertions defines the structural basis for the distinct activities of the polysaccharide-specific PmeA and the oligosaccharide-specific PmeB (Eklöf *et al.*, 2009). The open active-site cleft of *Ye*CE8 presented here indicates that *Ye*CE8 is also a PmeA-type PME and therefore active on large polymeric substrates (Fig. 2*b*).

### 3.3. Pectin utilization within *Yersinia*

The presence of pectin-utilization pathways within the genomes of enteropathogenic species from Enterobacteriaceae has been described previously (Rodionov *et al.*, 2004; Abbott & Boraston, 2008). The biological significance of the utilization of a structural plant cell-wall polysaccharide as an energy source by these microbes, however, remains to be determined. Although subtle differences in the complement of biocatalysts and their predicted cellular locations are noted between species such as *Salmonella*, *Shigella*, *E. coli*, *Klebsiella* and *Yersinia*, several features are absolutely conserved, including a KdgR repressor protein, a member of the KdgM outer membrane porin family, a CE8 and an intact cytoplasmic pathway (Hugouvieux-Cotte-Pattat *et al.*, 1996; Rodionov *et al.*, 2004; Abbott & Boraston, 2008). Determining when pectin-utilization pathways are activated during enteropathogenic life cycles may be a key discovery for understanding the role of pectin utilization in environmental persistence, food-crop contamination or colonization of the host gut (Abbott *et al.*, 2010). In this light, the presence of a conserved pathway within the zoonotic *Y. pestis*, which is not known to pass through the host digestive system, is intriguing.

The potential role of a subclade of CE8s in a biological process other than pectin demethylesterification suggests that the CE8 homologue is not essential for pectin harvesting in enteric bacteria (Eklöf *et al.*, 2009). Insights into the evolutionary history of CE8s found within a group of enteropathogens from Enterobacteriaceae, including *Klebsiella*, *Erythrobacter*, *Citrobacter*, *Salmonella* and *Shigella*, revealed that this group of CE8s arose from the PmeB isozyme (Fig. 3) and display notable functional differences from PmeAs, including (i) a lipidated anchor, (ii) a remodelled active-site cleft and (iii) an acid–base catalyst that is mutated from an aspartate to an asparagine (see Supplementary Material; Eklöf *et al.*, 2009). The phylogenetic analysis presented here indicates that CE8s found within the genus *Yersinia* contain highly conserved PmeA-like homologues, as opposed to the PmeB-like homologues in other enteric bacteria, and retain the structural signatures required for

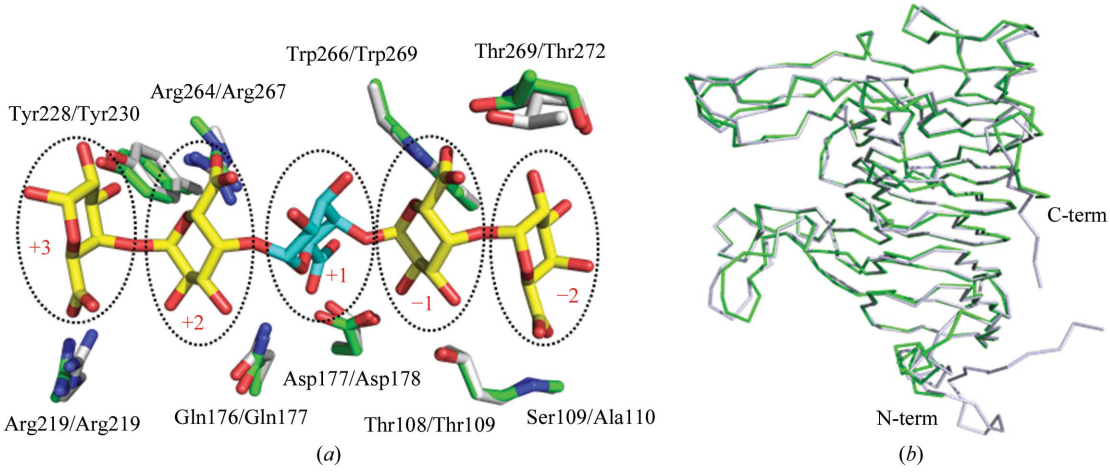


**Figure 2**
Comparison of the functional groups involved in direct carbohydrate interactions within the active sites of *Ye*CE8 (green) and *Dd*CE8 (grey). The amino acids are shown as sticks and labelled as in *Ye*CE8/*Dd*CE8. Five of the six sugar residues of the $GalA_6$ product (PDB entry 2ntb) are displayed as yellow sticks; the GalA residue with the scissile methyl group is coloured cyan. Subsites are indicated by black dashed ellipses and are numbered in red. The putative *Ye*CE8 nucleophile (Asp199) is not shown, but is structurally conserved with the homologous *Dd*CE8 residue (Asp199). (*b*) Ribbon representation of superimposed *Ye*CE8 (green; PDB entry 3uw0) and *Dd*CE8 (grey; PDB entry 2ntb) displaying the open active site of the PmeA-type PMEs.

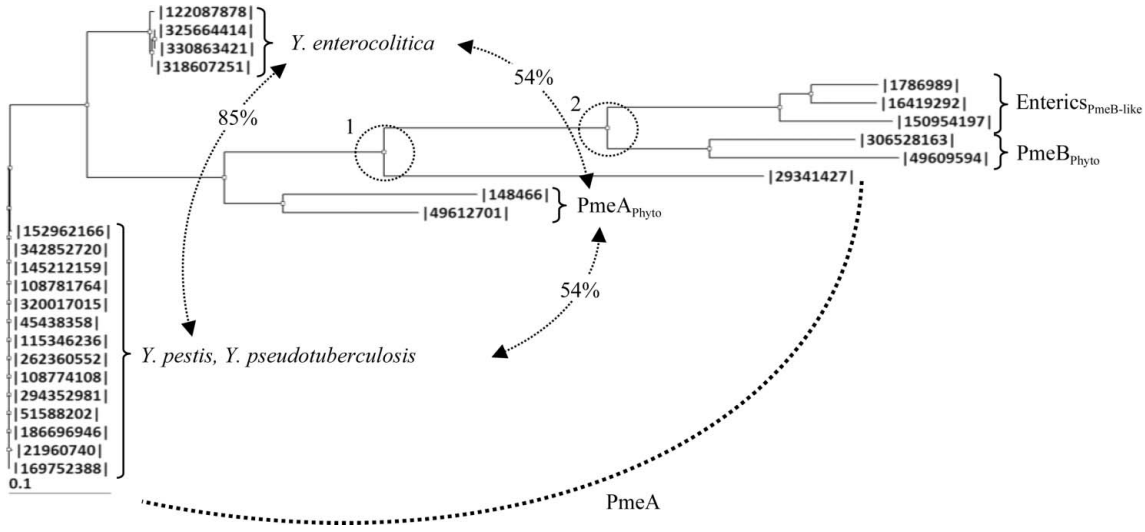


**Figure 3**
Phylogram of CE8 enzymes from *Yersinia* and bacterial phytopathogens and enteropathogens. Neighboring-joining phylogram of CE8s from *Y. pestis* (342852720, A1122; 145212159, Pestoides F; 108781764, Antiqua; 320017015, biovar Mediaevalis str. Harbin 35; 5438358, biovar Microtus str. 91001; 115346236, CO92; 262360552, D106004; 21960740, KIM 10; 108774108, Nepal516; 294352981, Z176003), *Y. pseudotuberculosis* (152962166, IP_31758; 51588202, IP_32953; 186696946, PB1/+; 169752388, YPIII) and *Y. enterocolitica* [122087878, subsp. *enterocolitica* 8081; 325664414, subsp. *palearctica* 105.5R(r); 318607251, subsp. *palearctica* Y11; 330863421, W22703] strains with (1) PmeA from *B. thetaiotaomicron* (29341427) and the phytopathogens *D. dadantii* 3937 (148466) and *Pectobacterium atrosepticum* SCRI1043 (49612701), (2) PmeB from *D. dadantii* 3937 (306528163) and *P. atrosepticum* SCRI1043 (49609594) and (3) PmeB-like enzymes from the enteropathogens *K. pneumonia* subsp. *pneumonia* MGH78578 (150954197), *S. enterica* subsp. *enterica* serovar Typhimurium str. LT2 (16419292) and *E. coli* str. K-12 substr. MG1655 (1786989). The relatedness (represented as percentage identity) between the *Y. enterocolitica*, $PmeA_{Phyto}$ and *Y. pestis*/*Y. psudotuberculosis* subclades are labelled. Two significant divergences separating the *Yersinia* enzymes from the other PMEs and the PmeAs from the PmeBs are indicated by dashed circles and labelled.

polymeric pectin demethylesterification by *Dd*CE8 (Fig. 3; Supplementary Material). This observation is consistent with the genomes of *Yersinia* displaying the most developed pectin-utilization pathways of any enteropathogen from the Enterobacteriaceae. Indeed, *Y. pestis*, *Y. pseudotuberculosis* and *Y. enterocolitica* each contain an exo-polygalacturonase (*Ye*GH28) and two pectate lyases (*Ye*PL2A and *Ye*PL2B) that are also found in plant-cell macerating phytopathogens (Abbott & Boraston, 2008; Rodionov *et al.*, 2004; Hugouvieux-Cotte-Pattat *et al.*, 1996). Importantly, the presence of a *bone fide* pectin methylesterase supports the idea that pectin metabolism may play a more significant role in the biological fitness or transmission of *Yersinia* than in other related enteric bacteria.

This work was funded by a grant from the Natural Sciences and Engineering Research Council of Canada. ABB is a Canada Research Chair in Molecular Interactions and a Michael Smith Foundation for Health Research Scholar.

## References


Abbott, D. W. & Boraston, A. B. (2008). *Microbiol. Mol. Biol. Rev.* **72**, 301–316.
Abbott, D. W., Gilbert, H. J. & Boraston, A. B. (2010). *J. Biol. Chem.* **285**, 39029–39038.
Battye, T. G. G., Kontogiannis, L., Johnson, O., Powell, H. R. & Leslie, A. G. W. (2011). *Acta Cryst.* D**67**, 271–281.
Cantarel, B. L., Coutinho, P. M., Rancurel, C., Bernard, T., Lombard, V. & Henrissat, B. (2009). *Nucleic Acids Res.* **37**, D233–D238.
Chen, V. B., Arendall, W. B., Headd, J. J., Keedy, D. A., Immormino, R. M., Kapral, G. J., Murray, L. W., Richardson, J. S. & Richardson, D. C. (2010). *Acta Cryst.* D**66**, 12–21.
DeLano, W. L. (2002). *PyMOL*. http://www.pymol.org.
Di Matteo, A., Giovane, A., Raiola, A., Camardella, L., Bonivento, D., De Lorenzo, G., Cervone, F., Bellincampi, D. & Tsernoglou, D. (2005). *Plant Cell*, **17**, 849–858.
Eklöf, J. M., Tan, T.-C., Divne, C. & Brumer, H. (2009). *Proteins*, **76**, 1029–1036.
Emsley, P. & Cowtan, K. (2004). *Acta Cryst.* D**60**, 2126–2132.
Evans, P. (2006). *Acta Cryst.* D**62**, 72–82.
Fries, M., Ihrig, J., Brocklehurst, K., Shevchik, V. E. & Pickersgill, R. W. (2007). *EMBO J.* **26**, 3879–3887.
Gasteiger, E. H. C., Gattiker, A., Duvaud, S., Wilkins, M. R., Appel, R. D. & Bairoch, A. (2005). *The Proteomics Protocols Handbook*, edited by J. M. Walker, pp. 571–607. Totowa: Humana Press.
Holm, L. & Rosenström, P. (2010). *Nucleic Acids Res.* **38**, W545–W549.
Hugouvieux-Cotte-Pattat, N., Condemine, G., Nasser, W. & Reverchon, S. (1996). *Annu. Rev. Microbiol.* **50**, 213–257.
Jenkins, J., Mayans, O., Smith, D., Worboys, K. & Pickersgill, R. W. (2001). *J. Mol. Biol.* **305**, 951–960.
Jenkins, J. & Pickersgill, R. (2001). *Prog. Biophys. Mol. Biol.* **77**, 111–175.
Johansson, K., El-Ahmad, M., Friemann, R., Jörnvall, H., Markovic, O. & Eklund, H. (2002). *FEBS Lett.* **514**, 243–249.
Kazemi-Pour, N., Condemine, G. & Hugouvieux-Cotte-Pattat, N. (2004). *Proteomics*, **4**, 3177–3186.
Murshudov, G. N., Skubák, P., Lebedev, A. A., Pannu, N. S., Steiner, R. A., Nicholls, R. A., Winn, M. D., Long, F. & Vagin, A. A. (2011). *Acta Cryst.* D**67**, 355–367.
Pelloux, J., Rustérucci, C. & Mellerowicz, E. J. (2007). *Trends Plant Sci.* **12**, 267–277.
Read, R. J. (1986). *Acta Cryst.* A**42**, 140–149.
Rodionov, D. A., Gelfand, M. S. & Hugouvieux-Cotte-Pattat, N. (2004). *Microbiology*, **150**, 3571–3590.
Shevchik, V. E., Condemine, G., Hugouvieux-Cotte-Pattat, N. & Robert-Baudouy, J. (1996). *Mol. Microbiol.* **19**, 455–466.
Vagin, A. & Teplyakov, A. (2010). *Acta Cryst.* D**66**, 22–25.